BORON 3 (1), 51 - 62, 2018

BOR DERGİSİ

JOURNAL OF BORON

http://dergipark.gov.tr/boron

Synthesis of Fe-Fe_2B catalysts via solvothermal route for hydrogen generation by hydrolysis of $NaBH_4$

Mustafa Barış[1], Tuncay Şimşek[2], Hatice Taşkaya[3], Arun K. Chattopadhyay[4]

[1]Eti Maden Works General Management, 06105 Ankara, Turkey, ORCID ID, orcd.org/0000-0002-2119-0697
[2]Mersin University, Department of Industrial Design, Mersin 33343, Turkey, ORCID ID, orcd.org/0000-0002-4683-0152
[3]Middle East Technical University, Department of Chemical Engineering, 06800 Ankara, Turkey, ORCID ID, orcd.org/ 0000-0001-6089-8711
[4]Etimine USA Inc., 1 Penn Center West, Suite-400, PA15276, Pittsburgh, USA, ORCID ID, orcd.org/0000-0001-5095-6463

ARTICLE INFO

Article history:
Received 31 October 2017
Received in revised form 29 December 2017
Accepted 26 January 2018
Available online 26 March 20178

Research Article

DOI: 10.30728/boron.348291

Keywords:
Fe_2B,
Nanocrystal
Solvothermal Method,
Hydrogen production

ABSTRACT

In this study, iron sulfate ($FeSO_4$) and sodium borohydride ($NaBH_4$) were used to synthesize Fe-Fe_2B nanocrystals via the solvothermal route. Synthesis of Fe-Fe_2B nanocrystals was carried out under Argon (Ar) gas atmosphere with aqueous solutions of $FeSO_4.7H_2O$ and $NaBH_4$ at various concentrations and reaction time. The phases and microstructures of nanocrystals thus formed were characterized by X-Ray diffraction (XRD) spectroscopy and scanning electron microscopy (SEM). Surface areas of nanocrystals were measured by a surface area and pore-size analyzer using nitrogen adsorption-desorption method together with Brunauer-Emmett-Teller (BET) equation. The vacuum dried nanoparticles were calcined under both Ar and air at 500 ºC. Nano-cylindrical structures of Fe-Fe_2B were observed when calcinated under Ar atmosphere; whereas more irregular shaped particles were noticed when calcinated under air. The surface areas of Fe-Fe_2B were determined as 12 m^2/g, 5.5 m^2/g and 16.5 m^2/g, for vacuum dried, Ar-calcined and O_2-calcined products respectively. The catalytic effect of those nano-particles to generate hydrogen was studied by determining reaction rate of decomposition of $NaBH_4$ in aqueous alkaline solution. The catalytic activity was investigated by systematic variation of three parameters (1) the amount of Fe-Fe_2B, (2) the concentration of $NaBH_4$ and (3) the concentration of NaOH. The effect of temperature on the catalytic activity was also studied separately for the most effective composition by varying the temperature from 25 to 70 °C. It was noticed that the catalytic activity of vacuum dried nanocrystals was the highest. The catalytic activity was found to increase with the increase in $NaBH_4$ concentration and decrease with the increase in NaOH concentration. The influence of temperature studied with 0.01 g of Fe-Fe_2B in 1 % w/w $NaBH_4$ solution showed that the rate of hydrogen generation could be increased almost 5 times more by varying the temperature from 25 °C to 70 °C.

1. Introduction

Besides their characteristic high hardness properties, high melting points, excellent electrical and thermal conductivities, and corrosion and abrasion resistance properties [1-5], metal borides are also used as catalysts for an efficient hydrogen generation in the fuel cell [6-9].

For fuel cell applications, the use of metal borides is particularly important for catalyzing the decomposition of alkaline borohydrides, such as sodium borohydride ($NaBH_4$) [10-19], lithium boron hydride ($LiBH_4$) [20-21], potassium borohydride (KBH_4) [22-23] and ammonia borane (NH_3BH_3) [24-28].

Among all borohydrides studied, $NaBH_4$ is regarded as the most promising and reliable one because of its high H_2 storage capacity per mass (10.8 wt %), for its well-controlled H_2 generation, its good storage and oxidation stability; moreover, it is non-toxic and non-flammable. In the presence of any heterogeneous or homogenous catalyst, aqueous solutions of sodium borohydride ($NaBH_4$) can undergo hydrolytic decomposition to produce H_2 gas at room temperature. During hydrolysis, H_2 is produced together with the formation of sodium metaborate ($NaBO_2$) as shown in Eq. 1 [12-13,15,17].

$$NaBH_4 + 2H_2O \rightarrow NaBO_2 + 4H_2 \qquad (1)$$

For catalysis of $NaBH_4$, the use of finely divided metal catalysts are often emphasized elsewhere, particularly the use of Pd [29-32], Pt [33-36] and Ru [37-41]. However, despite their excellent catalytic efficiencies, the use of those metal catalysts is highly cost prohibitive,

---

*Corresponding author: mustafabaris@etimaden.gov.tr which makes their usage for fuel-cells applications highly uneconomical. For that matter use of suitable metal borides of finer particle sizes, nano-particles for example, are highly desirable.

Nanoparticles of metal borides of various crystallite size and shapes can be produced by self-propagating high-temperature synthesis [42], molten salt method [43], electrolysis method [44], chemical vapor deposition [45], carbothermal method [46], sol-gel [47-48], mechanochemical [49] and solvothermal methods [50]. However, solvothermal methods are preferred over the other methods due to their ability to produce nanoparticles of uniform shapes and sizes. Various studies about the production of metal borides via solvothermal routes are well elaborated in the literatures [51-55]. The solvothermal synthesis of magnetic metal borides and their studies on catalytic activities such as Fe_2B, Co_2B, and Ni_2B and draws special attention in this regard [56-59].

The present work mainly focuses on the study of nano-ironboride catalyst as a cost-effective alternate for the hydrolysis of $NaBH_4$. To the best of our knowledge, the comparative catalytic activities of vacuum dried versus Ar-calcined and O_2-calcined Fe-Fe_2B nanoparticles were investigated for the first time for the hydrolysis of $NaBH_4$. This study was pursued by essentially varying three parameters, (a) the amount of catalyst, (2) the concentrations of $NaBH_4$, and (3) the concentration of NaOH. The effect of temperature on the rate of reaction was also investigated by varying the temperature from 25-70 **°C** for a fixed concentration of Fe-Fe_2B and $NaBH_4$.

2. Materials and Methods

2.1. Catalysts preparation and calcination treatment

Iron sulfate ($FeSO_4$, 99%, Aldrich Chem. Corp.) and sodium borohydride ($NaBH_4$, 98%, Aldrich Chem. Corp.) are used as Fe and B sources. Sodium hydroxide (NaOH, 97%, Aldrich Chem. Corp.) is used as a buffer. All experiments were performed in distilled-deionized water and under Argon (%99.999) gas atmosphere. Three-necked glass reactor (500 ml) and magnetic stirrer (MTops HSD180) are used in experiments.

The preparation of Fe-Fe_2B catalyst performed by the chemical reduction of different $FeSO_4$ and $NaBH_4$ concentration given in Table 1. The first set of experiments were carried out in aqueous medium for 3, 12, 60 and 120 min for determination of the optimum reaction time while second set of experiments were performed for determination of the $FeSO_4$ and $NaBH_4$ concentration. Firstly, $FeSO_4$ was dissolved in cold distilled water and this aqueous water solution was introduced in to three-necked glass reactor. To prevent formation of unwanted phases, experiments were carried out in ice bath at about 4 °C. The main solution was stirred with magnetic stirrer for thermal equilibrium for 10 minutes under Ar gas atmosphere. Secondly, alkaline $NaBH_4$ was dissolved in 20 mL distilled water and added to main solution drop-by-drop carefully. As soon as $NaBH_4$ was added to solution, black nanocrystals were obtained. When the reactions were completed, particles were washed with distilled water for several times to remove residual ions. Particles were centrifuged to separate from liquid to solid and dried in vacuum (Memmert VO400) at 20 mbar and 70 °C for 12 h. Then, vacuum dried nanoparticles were calcined at 500 °C under Ar and O_2 for 2 hours with a heating rate of 2 °C/min. respectively.

2.3. Catalyst characterization

Phases of synthesized samples are characterized by X-Ray diffraction spectrophotometer (XRD, Rigaku, D/MAX-2200 with CuKα, (λ=1.5408 ºA) at 40 kV working voltage, 30 mA current, 2-90° 2θ angle interval and 4°/min scan rate. Microstructure and morphology studies were performed by scanning electron microscopy (SEM, FEI Quanta 200F). Surface area of nanoparticles were measured by a surface area and pore-size analyzer (Quantaochrome, Nova 220E) using nitrogen adsorption-desorption method together with Brunauer-Emmett-Teller (BET) equation.

2.4. Catalytic activity runs

H_2 generation capacity of nanocrystals by the hydrolysis of $NaBH_4$ were determined in a pyrex glass reactor equipped with an apparatus capable of measuring H_2 evolution by the water-displacement method. H_2 generation system was shown in Figure 1. Typically, 10 mL distilled water and alkaline $NaBH_4$ solution was poured in a flask and then catalyst was added to solution under magnetic stirring at 700 rpm. Then, the volume of H_2 released was measured by opening the valve.

Table 1. Parameters of catalysis preparation.

Exp. No	$FeSO_4.7H_2O$ solution		$NaBH_4$ solution		Addition time (s)	Reaction time (min)	Magnetic stirring (rpm)
	$FeSO_4.7H_2O$ (g)	H_2O (ml)	$NaBH_4$ (g)	H_2O (ml)			
1	0.795	180	0.332	20	30	3-12-60-120	300
2	1.590		0.644				
3	3.180		1.289				

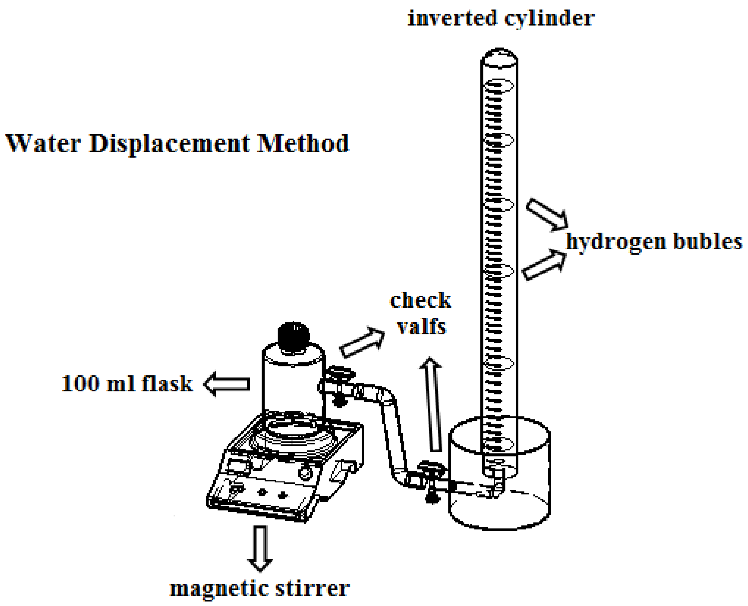

Figure 1. H_2 production system.

In order to investigate the catalytic activity of Fe-Fe_2B catalyst for the hydrolysis of $NaBH_4$, five different sets of experiments were performed in the aqueous medium of $NaBH_4$. The parameters used in the H_2 generation experiments are shown in Table 2. The effects of calcination, amount of catalyst used, concentrations of $NaBH_4$ and NaOH, and the temperature of reaction were investigated in the hydrogen generation experiments. In the first set of experiments, vacuum dried (0.01 g) and crystalline powders (0.01 g) were used as catalyst for H_2 generation by the hydrolysis of $NaBH_4$ (1 % w/w, 0.1 g) in aqueous media (10 mL distilled water). In the second set of experiments, hydrolysis reaction was carried out with various amount of catalysts (0.01, 0.02, 0.05, 0.1 g) at constant $NaBH_4$ concentration (1 % w/w, 0.1 g). In the third set of experiments, the amount of catalyst kept constant as 0.01 g and $NaBH_4$ concentration varied in the range of 1, 2, 5 and 10 % w/w. In the fourth set of experiments, concentration of NaOH was varied from 0.1-2 % w/w while $NaBH_4$ concentration was kept constant at 1 % w/w in the presence of 0.01 g of catalyst. In the fifth set of experiments, hydrolysis reaction were conducted by varying the reaction temperature from 25-70 °C.

3. Results and discussion

3.1. Phases and microstructural characterization of synthesized nanoparticles

The XRD pattern of starting materials of $FeSO_4$ is given in Figure 2. It can be noticed that the starting material, $FeSO_4$, showed the peaks for $FeSO_4.4H_2O$ (ICDD Card No: 00-016-0699) and $FeSO_4.7H_2O$ (ICDD Card No: 01-072-1106).

Iron boride catalyst was obtained by reduction of $FeSO_4$ with $NaBH_4$ in aqueous medium under Ar atmosphere. Expected reactions were given in Eq. 2 [60].

$$4FeSO_4 + 8NaBH_4 + 18H_2O \rightarrow 2Fe_2B + 6B(OH)_3 + 25H_2 + 4Na_2SO_4 \quad (2)$$

Fe^{++} reacts with $NaBH_4$ quickly to form Fe_2B, and H_2, Na_2SO_4 and $B(OH)_3$ as reaction byproducts. Fe-Fe_2B nanocrystals were formed by using alkaline $NaBH_4$ solution for the reaction with aqueous $FeSO_4.7H_2O$ solution. Synthesis of Fe-Fe_2B nanocrystals was monitored over a reaction time period 0-120 min in order to determine the effect of reaction time on the final phase structure and particle morphologies of Fe-Fe_2B. It was seen that within the first 3 minutes H_2 was released

Table 2. Parameters of catalytic activity experiments.

Set	Catayst type*	Amount of Catayst (g)	$NaBH_4$ concent. (wt%)	NaOH concent. (wt%)	Tempereature (°C)
I	A/Ar/O_2	0.01	1	-	25
II	A	0.01/0.02/0.05/0.1	1	-	25
III	A	0.01	1/2/5/10	-	25
IV	A	0.01	1	0.1/0.5/1/2	25
V	A	0.01	1	-	25/30/35/40/45/50/60/70

*A:Amorphous, Ar:Ar calcined, O_2:O_2 Calcined

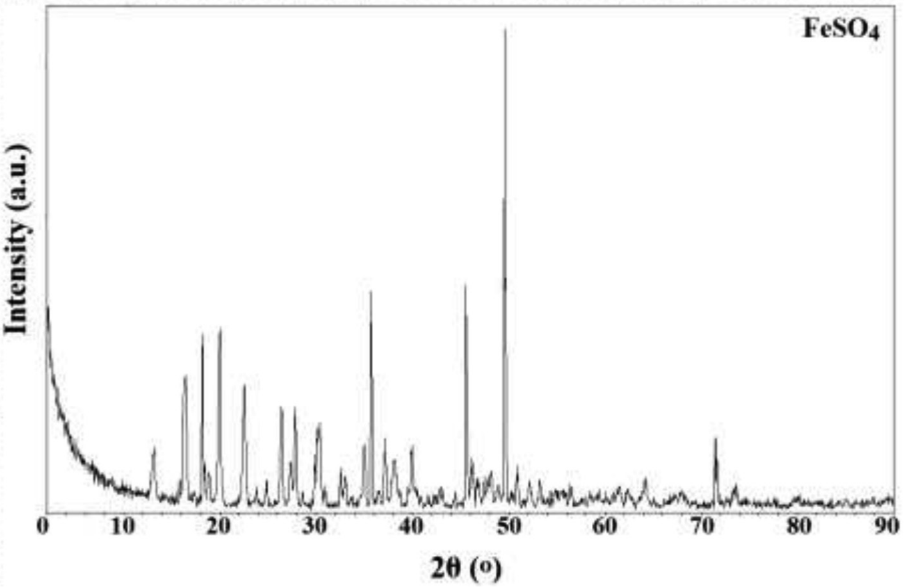

Figure 2. XRD pattern of starting materials of $FeSO_4$.

intensively, and then it slowed down and the reaction continued very slowly. It was noticed that up to 10 min, the black particles in the medium nearly became stable and very low amount of H_2 release was still observed. At the end of the 12th minute the reaction was complete, and H_2 release was not observed. The morphology of the nanoparticles in these experiments was monitored by keeping them over 120 minutes in the reaction mixtures. The nanoparticles with their prolonged stay under such conditions did not show any major changes in their morphology excepting some growth in their grain sizes. That's how the time the period for the synthesis of Fe-Fe_2B nanoparticles was optimized to 12 minutes. The particles synthesized over a time period of 12 min were centrifuged and dried under vacuum at 70°C for 12 h. Then, the samples were calcined under Ar and O_2 atmosphere for structural evolutions. XRD spectrum of vacuum dried, Ar-calcined and O_2-calcined Fe_2B nanoparticles obtained are shown in Figure 3.

It is seen from XRD pattern that the phase structures of vacuum dried samples were composed of Fe (ICDD Card No: 01-087-0722) phase before calcination. After drying the particles under vacuum and calcining at 500 °C for two hours under Ar and O_2, it appeared that the nano-particles comprised of Fe-Fe_2B and Fe-Fe_2O_3-Fe_3O_4 phases (Figures 3-b, and 3-c). XRD patterns of the vacuum dried particles is shown in Figure 3-a, and it exhibited the peaks of Fe phase around 2θ=44.76°, 65.16° and 82.53°. From Figure 3-b it was clearly seen that after calcination under Ar, the amorphous phases of Fe_2B were changed to crystalline Fe_2B (ICDD Card No: 01-089-1993) phases, and the nanopowder mixtures were composed of Fe and Fe_2B. The diffraction peaks around 2θ=24.61°, 35.09°, 42.51°, 45.00°, 50.47°, 56.93°, 74.16° and 80.69° are assigned to the diffraction of the Fe_2B phase. Unit cell refinements of iron phases were found and schematic representations of unit cells were also drawn in Figure 3. Cubic structure of Fe in *Im-3m* space group with the lattice parameters of of $a=b=c=2.8573$ Å and tetragonal structure of Fe_2B in *I4/mcm* space group with the lattice parameters of $a=b=5.1074$ Å and $c=4.2348$ Å and were confirmed with single phase unit cell refinements. For oxide phases, single unit cell refinements confirm the rhombohedra structure of Fe_2O_3 in *R-3c* space group with the lattice parameters of *a=b=5.0324 Å and* c*=13.7557 Å and cubic structure of* Fe_3O_4 in *Fd-3m* space group with the lattice parameters of $a=b=c=8.3414$ *Å*. The lattice parameters of

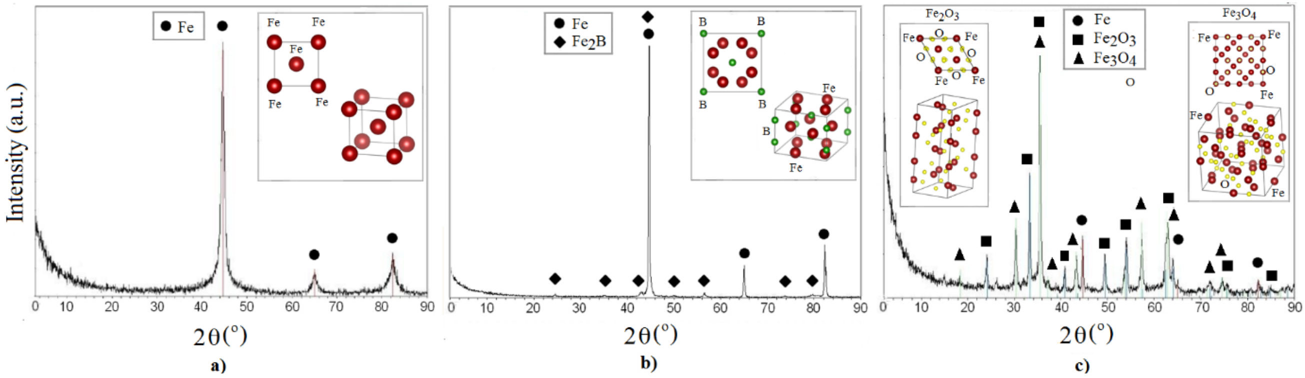

a) b) c)

Figure 3. XRD pattern and schematic representation of unit cell of a) Vacuum dried, b) Ar-calcined, c) O_2-calcined nanocrystals.

the catalyst were agreed fairly well with previous data [61-64]. In literature, the effect of calcination on the phases was investigated very intensively. Similar results were also reported in the study conducted by Bindai et al. They reported that the amorphous structure was transformed to crystalline structures after calcination process at 500 °C [65]. In another similar study, it is reported that vacuum dried samples structure was amorphous cobalt while the structures at elevated temperatures consisted of cobalt and cobalt boride [66]. By calcination under O_2, the phase structure of Fe_2B comprised oxides metallic Fe, Fe_2O_3 (ICDD Card No: 01-072-0469) and Fe_3O_4 (ICDD Card No01-088-0315) phase. As seen from XRD images given in Figure 2c, exposure of vacuum dried nanoparticles to air resulted in forming yellow-brown powder mixtures comprising Fe, Fe_2O_3 and Fe_3O_4. This can probably be best explained by the Eq. 3 given below. The continuous exposure to oxygen environment possibly led the Fe_2B to oxidize to form multiple oxide phases of Fe [67].

$$Fe_2B + 3/4O_2 \rightarrow 2Fe + 1/2B_2O_3$$
$$Fe_2B + O_2 \rightarrow Fe_xO_{x+1} + B_2O_3 \quad (3)$$

SEM analyses were carried out for morphological and microstructural observations. SEM images of the nanoparticles obtained with various $FeSO_4.7H_2O/NaBH_4$ concentrations are shown in Figure 4. As can be seen from this figure, Fe-Fe_2B nanoparticles obtained by different $FeSO_4$ initial concentration are clearly in nano-cylinder forms. It is also important to note that the size of the nano-cylinders increased with the increase in initial concentration of $FeSO_4$. The specific surface areas of powders were measured using BET method and surface areas were determined as 12, 12.5 and 15 m^2/g with the increased initial concentration of $FeSO_4$. It was also noticed that the nanocylinder structures were of irregular shapes with the sizes varying from 50-500 nm as the concentration of $FeSO_4$ increased.

Furthermore, comparative SEM images of Ar-calcined and O_2-calcined nanoparticles were given in Figure 4. It was also observed in Figure 5 that Ar-calcined nanoparticles were in nanocylinder form and particles were mostly agglomerated while O_2-calcined particles were composed of irregular shapes, and they were mostly found in aggregated forms with the particles sizes in the range of 40-300 nm. Surface area of nanocylinders of Ar-calcined and O_2-calcined were measured as 5.5 m^2/g and 16.5 m^2/g respectively.

3.2. Catalytic activities

Catalytic activities of vacuum dried, Ar-calcined and O_2-calcined powders by hydrolysis of $NaBH_4$ were determined in the first set of experiments. The catalytic activities of vacuum dried amorphous nanoparticles, Ar-calcined and O_2-calcined nanoparticles were given in Figure 6. The H_2 generation rate of vacuum dried amorphous nanoparticles with 0.01 g catalyst and 1 % w/w $NaBH_4$ concentration at room temperature was measured as 570 mL $H_2.g^{-1}.m^{-1}$. The H_2 generation rate of air-calcined Fe-Fe_2O_3-Fe_3O_4 and Ar-calcined Fe-Fe_2B catalysts were found as 450 mL $H_2.g^{-1}.m^{-1}$ and 400 mL $H_2.g^{-1}.m^{-1}$ respectively. These results are in agreement with the studies reported by Patel et al. It is reported that Hydrogen generation rate of heat treated samples was lower than amorphous samples [68]. It was determined that the vacuum dried nanoparticles hydrogen generation rate was the highest for hydro-

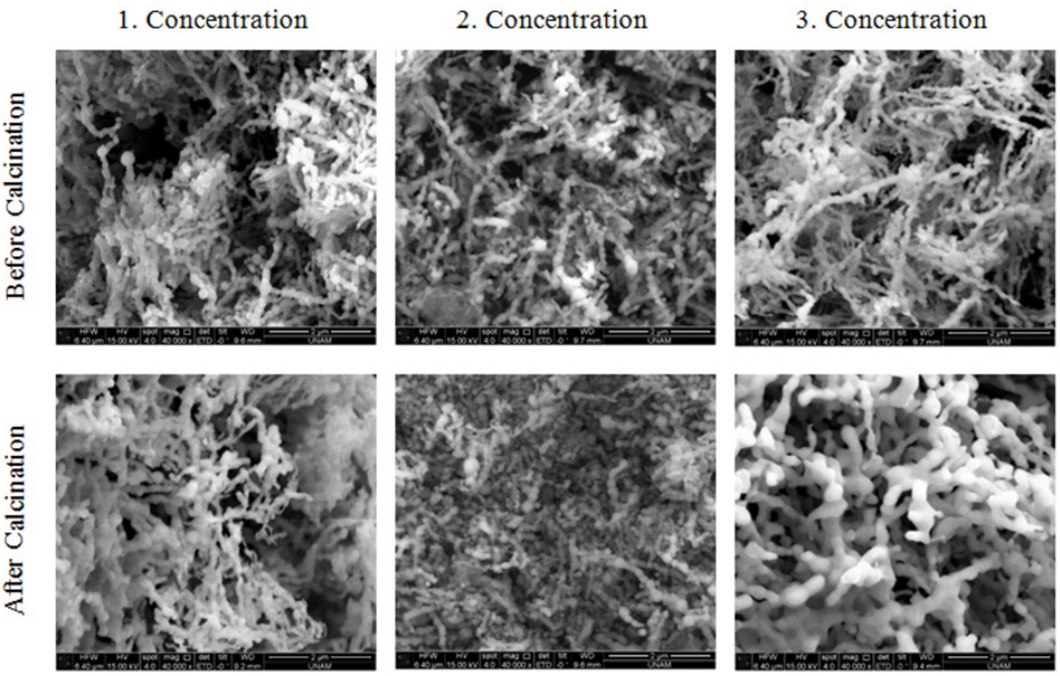

Figure 4. SEM images of vacuum dried nanoparticles obtained with $FeSO_4.7H_2O/NaBH_4$ concentration experiments.

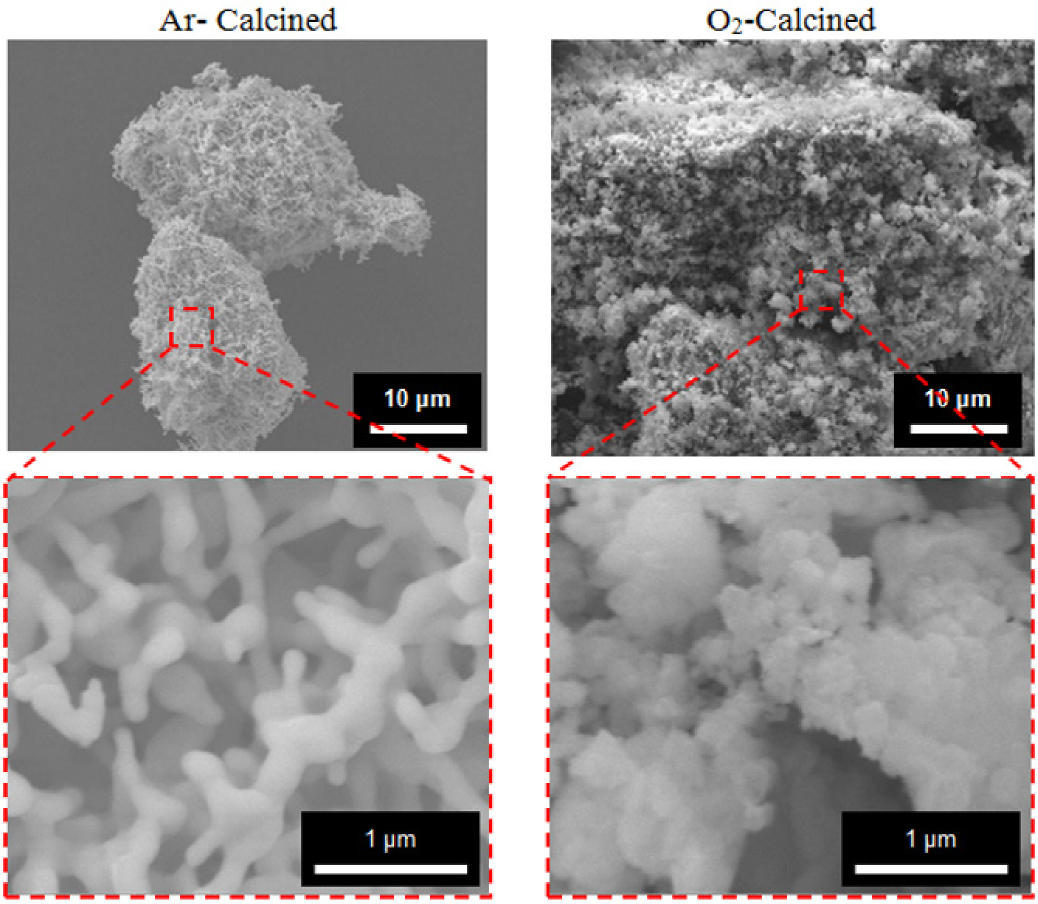

Figure 5. SEM images of Ar and O_2-calcined nanoparticles.

lysis of $NaBH_4$ in this study and so that vacuum dried nanoparticles were used in all subsequent catalytic activity experiments.

In the second set of experiments, the effect of the concentration of catalyst on the catalytic activity was investigated. In the second set the weight of the catalyst was progressively varied from 0.01, 0.02, 0.05 and 0.1g respectively keeping the concentration of $NaBH_4$ constant at 1wt% for the hydrolysis reaction. In all experiments of the second set 10 mL of distilled water was used at room temperature and with magnetic stirrer at 700 rpm. The H_2 generation rate of catalyst were given in Figure 7. As seen in Figure 7, as the amount of catalyst increased, the hydrogen generated rate increased. 220 mL H_2 was generated in 2700 s with 0.01 g catalyst. The same amount of H_2 was generated in 1800, 1080 and 720 s with 0.02, 0.05 and 0.1 g catalyst respec-

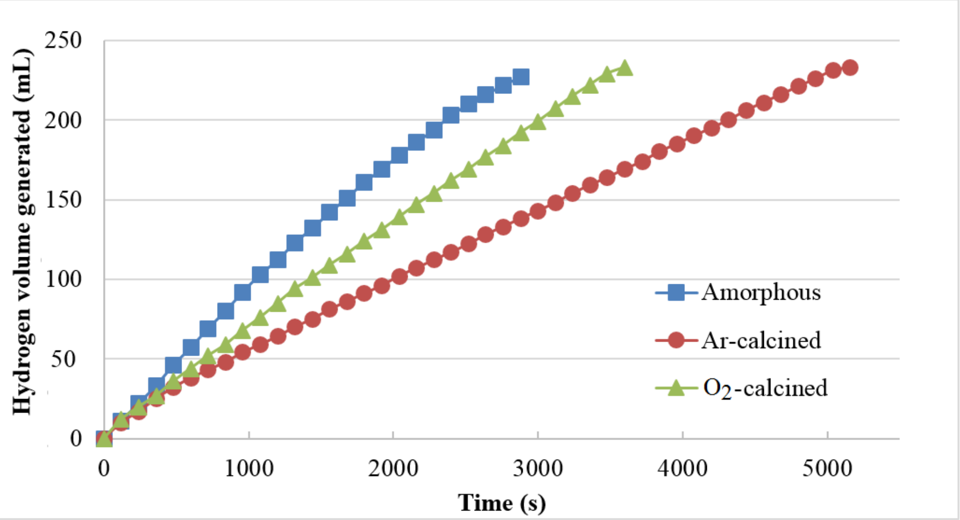

Figure 6. Catalytic activity of the vacuum dried, Ar-calcined and air-calcined powders, fixed $NaBH_4$ concentration of 1 w/w % and catalyst amount of 0.01 g.

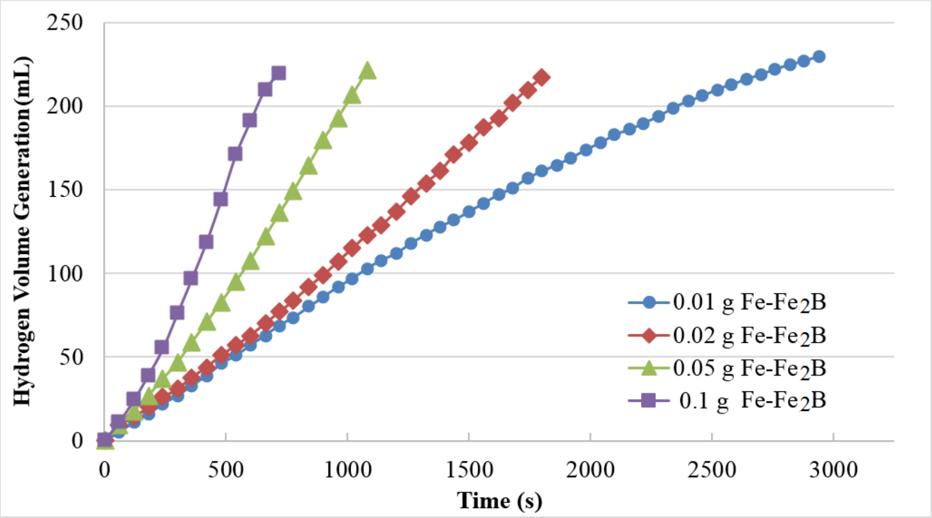

Figure 7. Influence of catalyst amount on the hydrogen generation rate at 25 °C, fixed $NaBH_4$ concentration of 1 w/w %.

tively. The similar results were observed with studies conducted by Sahiner et. al. as well. [69]. They reported that the increase in the amount of catalyst increases the rate of hydrogen production almost linearly for all the reactions performed under the same conditions.

In the third set of experiments, the effect of the $NaBH_4$ concentration of the medium, on the catalytic activity was investigated. The H_2 generation rates were given in Figure 8. In experiments with 0.01 g of vacuum dried nanoparticles in solution with 1 % w/w $NaBH_4$ concentration (0.1 g $NaBH_4$ + 10 mL H_2O), the hydrogen generation rate was measured as 570 mL H_2.g^{-1}.min^{-1}. By increasing the $NaBH_4$ concentration to 2, 5 and 10 % w/w, the H_2 generation rate was found as 1966, 4300 and 7700 mL H_2.g^{-1}.min^{-1}, respectively. It is noticed that the reaction rate was increased too fast with increasing of $NaBH_4$ concentration. The same results for up to % w/w 10 $NaBH_4$ concentration was found by Baydaroglu et al. They reported that the hydrogen generation rate increased as the $NaBH_4$ concentration was increased. Furthermore, it was claimed that high concentration of $NaBH_4$ more than % w/w 15 concentration leaded to increase in the viscosity and alkalinity of the reaction solution and the rate of hydrogen generation decreased probably due to solubility limitation of both $NaBH_4$ and $NaBO_2$ [10].

In the fourth set of experiments, the effect of different NaOH concentrations for H_2 generation performance of catalyst (0.01 g catalyst, 0.1 g $NaBH_4$ in 10 mL DDI) were investigated. The H_2 generation rate is given in Figure 9. It is known that $NaBH_4$ tend to the hydrolyze immediately. Therefore, NaOH is added to control the pH. An obvious decrease for $NaBH_4$ hydrolysis rate was observed with increasing NaOH concentration. It is known that $NaBH_4$ releases negligible amount of H_2 when it is contact with water. To avoid this release, the aqueous medium environment was controlled with NaOH concentration. Therefore, the effect of NaOH concentration on the catalytic activity was determined with various amount of NaOH concentrations. The H_2

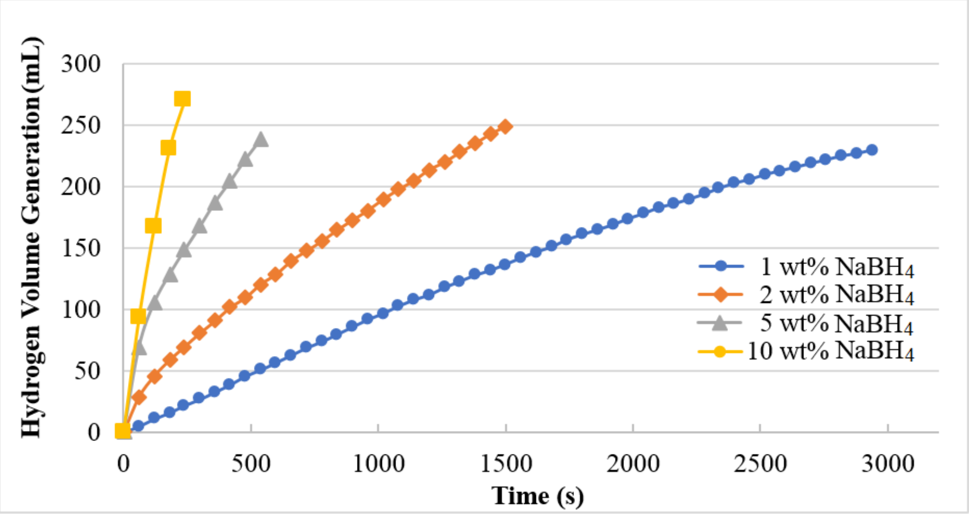

Figure 8. Influence of $NaBH_4$ concentration on the the hydrogen generation rate at 25 °C, fixed catalyst amount of 0.01 g.

production rate of 0.01 g of catalyst in the concentration of 0.1 % w/w $NaBH_4$ solution (0.1g $NaBH_4$ + 10 mL H_2O) at room temperature without addition of NaOH solution was measured as 570 mL H_2.g^{-1}.m^{-1}. It was found that catalytic activity rate was decreased when the NaOH was added to solution. H_2 generation rate of % w/w 0.1 NaOH concentration was 140 mL H_2.g^{-1}.m^{-1} while no measurable catalytic activity was detected for the first 20 minutes with 0.5 % w/w NaOH concentration. It was determined that after the 20 th minute, the catalytic activity started and H_2 generation rate was 230 mL H_2.g^{-1}.m^{-1}. No catalytic activity was observed for the first 24 min with 1 % w/w NaOH solution. Catalytic activity was started after 24 min and H_2 generation was found as 238 mL H_2.g^{-1}.m^{-1}. With experiments of 2 % w/w NaOH concentration, no catalytic activity was measured similarly in the first 72 min and catalytic activity was started from 72 min and H_2 generation rate was about 120 mL H_2.g^{-1}.m^{-1}. Similar results were also reported by studies conducted by Amendola et al. They claimed that at higher NaOH concentrations, water activity was reduced by the inhibiting effect of hydroxide ions. They thought that it occurred because of the ions, especially OH-, strongly complex water, thus decreasing the available free water needed for sodium borohydride hydrolysis. In another study, Liang et al. reported that increasing the NaOH concentration resulted in negative effect on hydrogen generation rate [70-71].

The effect of temperature on the catalytic activity is revealed with fifth set of experiments given in Figure 10. The increase in temperature has caused a significant increase in catalytic activity. In experiments with 0.01 g of Fe-Fe_2B vacuum dried nanoparticles at 25 °C in solution with 1 % w/w $NaBH_4$ concentration, the hydrogen production rate was 570 mL of H_2.g^{-1}.m^{-1}, while it reached to 1230 at 50 °C and 2700 mL H_2.g^{-1}.m^{-1} at 70 °C. As expected, increasing temperature increased H_2 production substantially and these results show that temperature is an important parameter for catalytic activity. As the temperature increased from 25 to 70 °C, the hydrogen generation rate increased from 570 to 2700 mL H_2.g^{-1}.m^{-1}. Many studies can be seen in the literature, about the increased hydrogen production rate of metal catalysts by increasing the temperature [13-16]. The hydrogen generation rate was increased with increasing temperature as expected. An important parameter of reaction kinetics, the activation energy (E_a) was determined by using the H_2 generation rates at varied temperature of solution in the range of 20-70 °C. The H_2 generation rate constant at various temperature was determined with the slope of fitting lines. The activation energy was calculated by the Arrhenius equation [4].

$$k = k_0 . e^{(-\frac{Ea}{RT})} \qquad (4)$$

Where k represents the reaction rate (mL.min^{-1}.g^{-1}), k_0 – the reaction constant (mL.min^{-1}.g^{-1}), E_a – the activation energy for the reaction (kJ.mol^{-1}), R – the gas constant (8.314 kJ.mol^{-1} K^{-1}) and T – the reaction temperature (K). The Arrhenius plot of lnk against to temperature (1/T) is given in Figure b. The activation Energy was calculated as 38 kj.mol^{-1} from the slope of straight line for the Fe-Fe_2B catalyst. It is known that the activation of chemical reaction was influenced by different parameters such as particle size, reaction temperature and the method of synthesis. Similar results were reported by Dinç et al. study. They reported that the activation energy of iron nanocluster for ammonia borane was calculated as 37 kj.mol^{-1} [72].

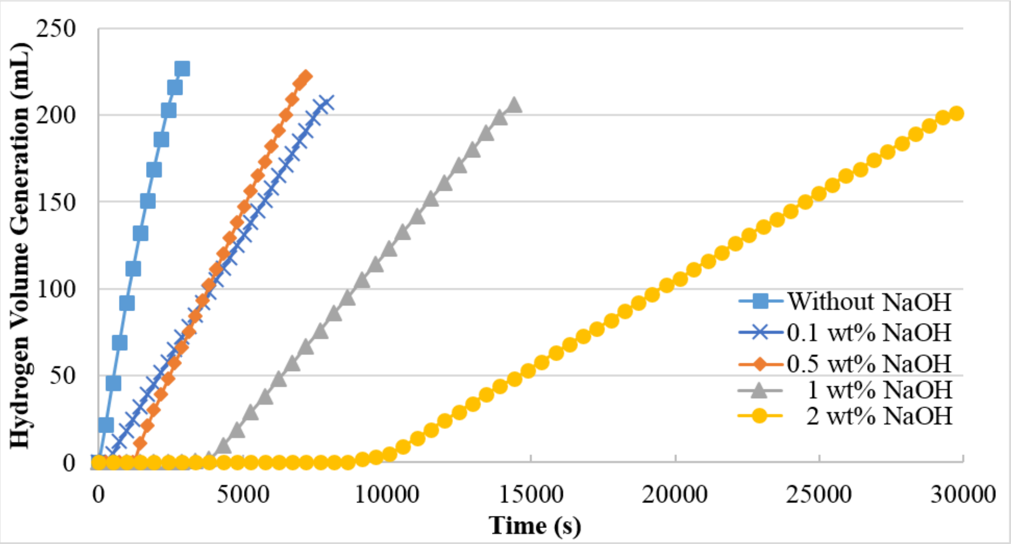

Figure 9. Influence of NaOH concentration on the the hydrogen generation rate at 25 °C, fixed $NaBH_4$ concentration of 1 w/w % and catalyst amount of 0.01 g.

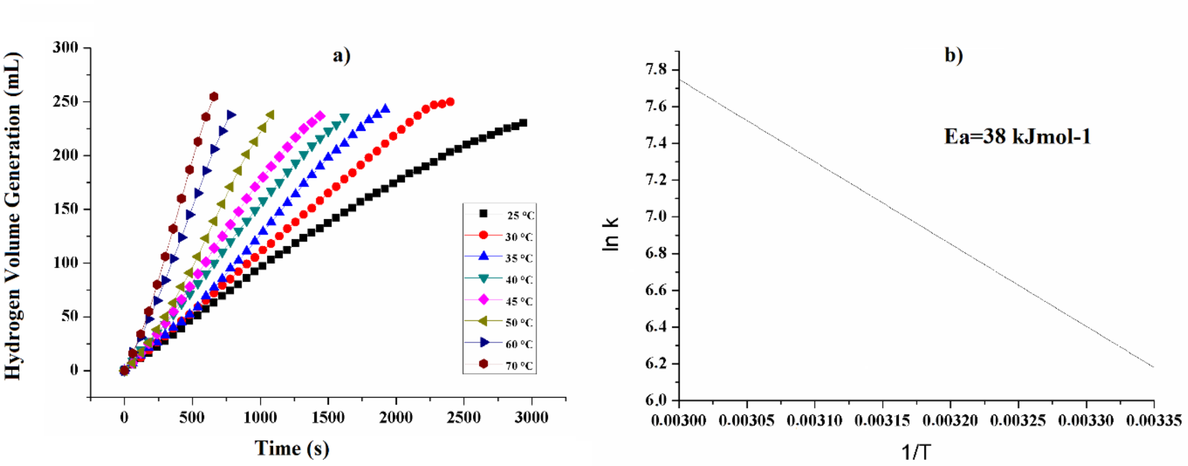

Figure 10. Influence of temperature on the hydrogen generation rate, fixed NaBH$_4$ concentration of 1 w/w % and catalyst amount of 0.01 g.

4. Conclusion

Fe-Fe$_2$B nanocylinder/nanocrystals were synthesized with various FeSO$_4$.7H$_2$O and alkaline NaBH$_4$ concentration in an aqueous medium. It is seen that vacuum dried nanoparticles were composed of Fe phase before calcination. After drying the particles under vacuum and then calcine at 500 ^{o}C for 2 hours in Ar and O$_2$, phase structures were comprised of Fe-Fe$_2$B and Fe-Fe$_2$O$_3$-Fe$_3$O$_4$ phases, respectively. It was found that increasing FeSO$_4$.7H$_2$O concentration the nanocylinders formed by calcination under Ar were of diameters between 50-500 nm. Whereas, the nanoparticles formed by calcination under O$_2$ were of irregular shapes and morphology. Surface areas were measured as 12m^2/g, 5.5 m^2/g and 16.5 m^2/g for the vacuum dried, Ar-calcined and O$_2$-calcined nanoparticles, respectively. The maximum H$_2$ generation rate was obtained as 2700 mL H$_2$.g^{-1}.m^{-1} at 70 °C by using amorphous Fe-Fe$_2$B with 1 % w/w of initial NaBH$_4$ concentration. Increasing the amount of catalysts and NaBH$_4$ concentration increased the H$_2$ production rate while increasing NaOH concentration dramatically decreased H$_2$ production rate.

Acknowledgements

The authors are very grateful to Eti Maden Works General Management for laboratory facilities usages.

References

[1] Yalaz N., Kocakuşak S., Kalafatoğlu E., İnorganik bor bileşikleri kaynak araştırması metal borürler, TÜBİTAK Marmara Bilimsel ve Endüstriyel Araştırma Enstitüsü, Kocaeli, 1-84 1988.

[2] Telle R., Boride and Carbide Ceramics, Materials Science and Technology, 11, Swain, M., VCH Publishers Inc., New York, 185-229, 1994.

[3] Lundstrom T., Structure, defects and properties of some refractory borides, Pure&Applied Chem., 57 (10), 1384, 1985.

[4] Schwetz K. A., Lipp A., Boron carbide, boron nitride, and metal borides, Ullmann's Encyclopedia of Industrial Chemistry, A4, Campbell, F. T., Pfefferkorn, R., Wiley-VCH, Weinheim, 303-306, 1985.

[5] Habashi F., Handbook of Extractive Metallurgy, Wiley-VCH, NewYork, 4, 1997.

[6] Krishnan P., Hsueh K. L., Yim S. D., Catalysts for the hydrolysis of aqueous borohydride solutions to produce hydrogen for PEM fuel cells, Appl. Catal., B, 77, 206-214, 2007.

[7] Patel N., Miotello A., Progress in Co-B related catalyst for hydrogen production by hydrolysis of boron-hydrides: A review and the perspectives to substitute noble metals, Int. J. Hydrogen Energy, 40, 1429-1464, 2015.

[8] Demirci U. B., Akdim O., Andrieux J., Hannauer J., Chamoun R., Miele P., Sodium Borohydride Hydrolysis as Hydrogen Generator: Issues, State of the Art and Applicability Upstream from a Fuel Cell, Fuel Cells, 10 (3), 335-350, 2010.

[9] Gupta S., Patel N., Miotello A., Kothari D.C., Cobalt-Boride: An efficient and robust electrocatalyst for Hydrogen Evolution Reaction, J. Power Sources, 279, 620-625, 2015.

[10] Baydaroglu F., Ozdemir E., Hasimoglu A., An effective synthesis route for improving the catalytic activity of carbon-supported Co-B catalyst for hydrogen generation through hydrolysis of NaBH$_4$, Int. J. Hydrogen Energy, 39, 1516-1522, 2014.

[11] Aydin M., Hasimoglu A., Ozdemir O.K., Kinetic properties of Cobalt-Titanium-Boride (Co-Ti-B) catalysts for sodium borohydride hydrolysis reaction, Int. J. Hydrogen Energy 41, 239-248, 2016.

[12] Edla R., Gupta S., Patel N., Bazzanella N., Fernandes R., Kothari D.C., Miotello A., Enhanced H$_2$ production from hydrolysis of sodium borohydride using Co$_3$O$_4$ nanoparticles assembled coatings prepared by pulsed laser deposition, Appl. Catal., A, 515, 1-9, 2016.

[13] Loghmani M. H., Shojaei A. F., Khakzad M., Hydrogen generation as a clean energy through hydrolysis of sodium borohydride over Cu-Fe-B nano powders: Effect of polymers and surfactants, Energy, 126 ,830-840, 2017.

[14] Wei Y., Meng W., Wang Y., Gao Y., Qi K., Zhang K., Fast hydrogen generation from $NaBH_4$ hydrolysis catalyzed by nanostructured Co-Ni-B catalysts, Int. J. Hydrogen Energy, 42, 6072-6079, 2017.

[15] Kojima Y., Suzuki K. I, Fukumoto K., Sasaki M., Yamamoto T., Kawai Y., Hayashi H., Hydrogen generation using sodium borohydride solution and metal catalyst coated on metal oxide, Int. J. Hydrogen Energy, 27, 1029 - 1034, 2002.

[16] Wang Y. P., Wang Y. J., Ren Q. L., Li L., Jiao L. F., Song D.W., Liu G., Han Y., Yuan H. T., Ultrafine Amorphous Co-Fe-B Catalysts for the Hydrolysis of $NaBH_4$ Solution to Generate Hydrogen for PEMFC, Fuel Cells, 10 (1) 132-138, 2010.

[17] Liang Z., Li Q., Li F., Zhao S., Xia X., Hydrogen generation from hydrolysis of $NaBH_4$ based on high stable NiB/$NiFe_2O_4$ catalyst, Int. J. Hydrogen Energy, 42, 3971-3980, 2017.

[18] Özsaçmacı G., Çakanyıldırım Ç., Gürü M., Co-Mn/TiO_2 catalyst to enhance the $NaBH_4$ decomposition, Boron 1 (1), 1 - 5, 2016.

[19] Şimşek T., Bariş M., Synthesis of Co_2B nanostructures and their catalytic properties for hydrogen generation , Boron 2 (1), 28 - 36, 2017.

[20] Kojima Y., Kawai Y., Kimbara M., Nakanishi H., Matsumoto S., Hydrogen generation by hydrolysis reaction of lithium Borohydride, Int. J. Hydrogen Energy, 29, 1213 - 1217, 2004.

[21] Kojima Y., Suzuki K. I., Kawai Y., Hydrogen generation from lithium borohydride solution over nano-sized platinum dispersed on $LiCoO_2$, J. Power Sources, 155, 325-328, 2006.

[22] Xu D., Wang H., Guo Q., Ji S., Catalytic behavior of carbon supported Ni-B, Co-B and Co-Ni-B in hydrogen generation by hydrolysis of KBH_4, Fuel Process. Technol., 92, 1606-1610 2011.

[23] Sahin Ö., Dolas H., Özdemir M., The effect of various factors on the hydrogen generation by hydrolysis reaction of potassium borohydride, Int. J. Hydrogen Energy, 32, 2330 - 2336, 2007.

[24] Cao N., Luo W., Cheng G., One-step synthesis of graphene supported Ru nanoparticles as efficient catalysts for hydrolytic dehydrogenation of ammonia borane, Int. J. Hydrogen Energy, 38, 11964-11972, 2013.

[25] Durap F., Zahmakıran M., Ozkar S., Water soluble laurate-stabilized ruthenium(0) nanoclusters catalyst for hydrogen generation from the hydrolysis of ammonia-borane: High activity and long lifetime, Int. J. Hydrogen Energy 34, 7223-7230, 2009.

[26] Wang C., Tuninetti J., Wang Z., Zhang C., Ciganda R., Salmon L., Moya S., Ruiz J., Astruc D., Hydrolysis of Ammonia-Borane over Ni/ZIF-8 Nanocatalyst: High Efficiency, Mechanism, and Controlled Hydrogen Release, J. Am. Chem. Soc., 139, 11610−11615, 2017.

[27] Mori K., Miyawaki K., Yamashita H., Ru and Ru−Ni Nanoparticles on TiO_2 Support as Extremely Active Catalysts for Hydrogen Production from Ammonia−Borane, ACS Catal., 6, 3128−3135, 2016.

[28] Qiu F., Li L., Liu G., Wang Y., Wang Y., An C., Xu Y., Xu C., Wang Y., Jiao L., Yuan H., In situ synthesized Fe-Co/C nano-alloys as catalysts for the hydrolysis of ammonia borane, Int. J. Hydrogen Energy, 38, 3241-3249, 2013.

[29] Jiang K., Xu K., Zou S., Cai W. B., B-Doped Pd Catalyst: Boosting Room-Temperature Hydrogen Production from Formic Acid−Formate Solutions, J. Am. Chem. Soc., 136, 4861−4864, 2014.

[30] Rakap M., The highest catalytic activity in the hydrolysis of ammonia borane by poly (N-vinyl-2-pyrrolidone)-protected palladium-rhodium nanoparticles for hydrogen generation, Appl. Catal., B, 163, 129-134, 2015.

[31] Akbayrak S., Kaya M., Volkan M., Özkar S., Palladium(0) nanoparticles supported on silica-coated cobalt ferrite:A highly active, magnetically isolable and reusable catalyst forhydrolytic dehydrogenation of ammonia borane, Appl. Catal., B,147, 387- 393, 2014.

[32] onbul Y., Akbayrak S., Ozkar S., Palladium(0) nanoparticles supported on ceria: Highly active and reusable catalyst in hydrogen generation from the hydrolysis of ammonia borane, Int. J. Hydrogen Energy, 41, 11154-11162, 2016.

[33] Clémençon D., Petit J.F., Demirci U.B., Xu Q., Miele P., Nickel- and platinum-containing core@shell catalysts for hydrogen generation of aqueous hydrazine borane, J. Power Sources, 260, 77-81, 2014.

[34] Wu C., Zhang H., Yi B., Hydrogen generation from catalytic hydrolysis of sodium borohydride for proton exchange membrane fuel cells, Catal. Today, 93-95, 477-483, 2004.

[35] Semaško M., Tamašiūnaitė L. T., Stalnionienė I., Želienė A., Vaičiūnienė J., Stanynienė B. S., Selskis A., Norkus E., Hydrogen Generation via Sodium Borohydride Hydrolysis Using Graphene Supported Platinum-Ruthenium-Cobalt Catalysts Prepared nu Microwave-Assisted Synthesis, ECS Trans., 68 (3), 37-44, 2015.

[36] Brack P Dann S. E., Wijayantha K. G., Heterogeneous and homogenous catalysts for hydrogen generation by hydrolysis of aqueous sodium borohydride ($NaBH_4$) solutions, Energy Sci. Eng., 3 (3),174-188, 2015.

[37] Cao N., Su J., Luo W., Cheng G, Graphene supported Ru@Co core-shell nanoparticles as efficient catalysts for hydrogen generation from hydrolysis of ammonia borane and methylamine borane, Catal. Commun., 43, 47-51, 2014.

[38] Cao N., Hu K., Luo W., Cheng G., RuCu nanoparticles supported on graphene: A highly efficient catalyst for hydrolysis of ammonia borane, J. Alloys Compd., 590, 241-246, 2014.

[39] Liang H., Chen G., Desinan S., Rosei R., Rosei F., Ma D., In situ facile synthesis of ruthenium nanocluster catalyst supported on carbon black for hydrogen generation from the hydrolysis of ammonia-borane, Int. J. Hydrogen Energy, 37, 17921-17927, 2012.

[40] Cao N., Liu T., Su J., Wu X., Luo W., Cheng G., Ruthenium supported on MIL-101 as an efficient catalyst for hydrogen generation from hydrolysis of amine boranes, New J.Chem., 38, 4032, 2014.

[41] Chowdhury A. D., Agnihotri N., De A., Hydrolysis of sodium borohydride using Ru-Co-Pedot nanocomposites as catalyst, Chem. Eng. J., 264, 531-537, 2015.

[42] Gadakary S., Khanra A. K., Veerabau R., Production of nanocrystalline TiB_2 powder through self-propagating high temperature synthesis (SHS) of TiO_2-H_3BO_3-Mg mixture, Advances in Applied Ceramics Structural, Functional and Bioceramics, Adv. Appl. Ceram., 113 (7) ,419-426, 2014.

[43] Wei Y., Liu Z., Ran S., Xi A., Yi T. F., Ji Y., Synthesis and properties of Fe-B powders by molten salt method, J. Mater. Res., 32 (4), 28, 883-889, 2017.

[44] Yin H., Tang D., Mao X., Xiao W., Wang D., Electrolytic calcium hexaboride for high capacity anode of aqueous primary batteries, J. Mater. Chem. A, 3, 15184-15189, 2015.

[45] Babar S., Kumar N., Zhang P., Abelson J. R., Dunbar A. C., Daly S. R., Girolami G. S., Growth Inhibitor To Homogenize Nucleation and Obtain Smooth HfB_2 Thin Films by Chemical Vapor Deposition, Chem. Mater., 25, 662-667, 2013.

[46] Qiu H. Y., Guo W. M., Zou J, Zhang G. J., ZrB_2 powders prepared by boro/carbothermal reduction of ZrO_2: The effects of carbon source and reaction atmosphere, Powder Technol., 217, 462-466, 2012.

[47] Liu Y., Geng R., Cui Y., Peng S., Chang X., Han K., Yu M., A novel liquid hybrid precursor method via sol-gel for the preparation of ZrB_2 films, Mater. Des., 128, 80-85, 2017.

[48] Cao Y., Zhang H., Li F., Lu L., Zhang S., Preparation and characterization of ultrafine ZrB_2-SiC composite powders by a combined sol-gel and microwave boro/carbothermal reduction method, Ceram. Int., 41, 7823-7829, 2015.

[49] Kudaka K., Lizumi K., Sasaki T., Okada S., Mechanochemical synthesis of MoB_2 and Mo_2B_5, J. Alloys Compd., 315, 104-107, 2001.

[50] Kelly J. P., Kanakala R., Graeve O. A., A Solvothermal Approach for the Preparation of Nanostructured Carbide and Boride Ultra-High-Temperature Ceramics, J. Am. Ceram. Soc., 93 (10) 3035-3038, 2010.

[51] Xiaochen S., Min D., Ming G., Bin Z., Weiping D., Solvent effects in the synthesis of CoB catalysts on hydrogen generation from hydrolysis of sodium borohydride, Chin. J. Catal., 34, 979-985, 2013.

[52] Gu Y., Qian Y., Chen L., Zhou F., A mild solvothermal route to nanocrystalline titanium diboride, J. Alloys Compd., 352, 325-327, 2003.

[53] Krishnan P, Advani S. G., Prasad A. K., Cobalt oxides as Co_2B catalyst precursors for the hydrolysis of sodium borohydride solutions to generate hydrogen for PEM fuel cells, Int. J. Hydrogen Energy, 33, 7095-7102, 2008.

[54] Wells S., Charles S. W., Morup S., Linderotht S., Wonterghem J. V., Larsent J, Madsent M. B., A study of Fe-B and Fe-CeB alloy particles produced by reduction with borohydride, J. Phys.: Condens. Matter, 1, 8199-8208, 1989.

[55] Gupta S., Patel N., Fernandes R., Kothari D.C., Miotello A., Mesoporous Co-B nanocatalyst for efficient hydrogen production by hydrolysis of sodium borohydride, Int. J. Hydrogen Energy, 38, 14685-14692 2013.

[56] Walter J. C., Zurawski A., Montgomery D., Thornburg M., Revankar S., Sodium borohydride hydrolysis kinetics comparison for nickel, cobalt, and ruthenium boride catalysts, J. Power Sources, 179, 335-339, 2008.

[57] Vernekar A.A., Bugde S. T., Tilve S., Sustainable hydrogen production by catalytic hydrolysis of alkaline sodium borohydride solution using recyclable Co-Co_2B and Ni-Ni_3B nanocomposites, Int. J. Hydrogen Energy, 37, 327-334, 2012.

[58] Manna J., Roy B., Vashistha M., Sharma P., Effect of Co^{+2}/BH^-_4 ratio in the synthesis of Co-B catalysts on sodium borohydride hydrolysis, Int. J. Hydrogen Energy, 39, 406-413, 2014.

[59] Hua D., Hanxi Y., Xinping A., Chuansin C., Hydrogen production from catalytic hydrolysis of sodium borohydride solution using nickel boride catalyst, Int. J. Hydrogen Energy, 28, 1095 - 1100, 2003.

[60] Mustapić M., Pajić D., Novosel N., Babić E., Zadro K., Cindrić M., Horvat J., Skoko Ž., Bijelić M., Shcherbakov A., Synthesis, Structural Characterization and Magnetic Properties of Iron Boride Nanoparticles with or without Silicon Dioxide Coating, Croat. Chem. Acta, 83 (3), 275-282, 2010.

[61] Choi C. J., Tolochko O., Kim B. K., Preparation of iron nanoparticles by chemical vapor condensation, Mater Lett, 56, 289– 294, 2002.

[62] Demortiere A., Panissod P., Pichon B. P, Pourroy G., Guillon D., Donnio B., Colin S. B., Size-dependent properties of magnetic iron oxide nanocrystals, Nanoscale, 3, 225-232, 2011.

[63] Xiao B., Xing J.D., Ding S.F, Su W., Stability, electronic and mechanical properties of Fe2B, Physica B, 403, 1723–1730, 2008.

[64] Barinov V. A., Tsurin V. A, Novikov S. I., Shein I. R., Surikov V. T., Short-Range Atomic Order in Fe2B Powders, The Physics Of Metals And Metallography, 103, 470–480, 2007.

[65] Dai H.B., Gao L.L., Liang Y., Kang X.D., Wang P., Promoted hydrogen generation from ammonia borane aqueous solution using cobalt-molybdenum-boron/nickel foam catalyst, J. Power Sources, 195, 307-312, 2010.

[66] Wu C., Wu F., Bai Y., Yi B., Zhang H., Cobalt boride catalysts for hydrogen generation from alkaline $NaBH_4$ solution, Mater. Lett., 59, 1748-1751, 2005.

[67] Glavee G. N., Klabunde K. J., Sorensen C. M., Hadjipanayis G. C., Chemistry of Borohydride Reduction of Iron(I1) and Iron(II1) Ions in Aqueous and Nonaqueous Media. Formation of Nanoscale Fe, FeB, and Fe_2B Powders, Inorg. Chem., 34, 28-35, 1995.

[68] Patel N., Fernandes R., Miotello A., Hydrogen generation by hydrolysis of $NaBH_4$ with efficient Co–P–B catalyst: A kinetic study, J. Power Sources, 188, 411-420, 2009.

[69] Sahiner N., Ozay O., Inger E., Aktas N., Controllable hydrogen generation by use smart hydrogel reactor containing Ru nano catalyst and magnetic iron nanoparticles, J. Power Sources, 196, 10105- 10111, 2011.

[70] Amendola S.C. Sharp-Goldman S.L., Janjua M.S., Spencer N.C., Kelly M.T., Petillo P.J., A safe, portable,

hydrogen gas generator using aqueous borohydride solution and Ru Catalyst, Int. J. Hydrogen Energy, 25, 969-75, 2000.

[71] Liang Y., Dai H.B., Ma L.P., Wang P., Cheng H.M., Hydrogen generation from sodium borohydride solution using a ruthenium supported on graphite catalyst, Int. J. Hydrogen Energy, 35, 3023-3028, 2010.

[72] Dinc M¸ Metin O, Ozkara S, Water soluble polymer stabilized iron(0) nanoclusters: A cost-effective and magnetically recoverable catalyst in hydrogen generation from the hydrolysis of sodium borohydride and ammonia borane, Catalysis Today, 183, 10– 16, 2012.